

Figure 2: (a) Aerosol optical depth (AOD) averaged for spring 2013 from MODIS, (b) same as (a) but from MISR, (c) same as (a) but from ECHAM6 - HAMMOZ BMAeroon simulation. (d) Comparison of simulated AOD (from BMAeroon) averaged for spring 2013 with AERONET observations at Gandhi college (GC; 25.81°N - 85.12°E), Kathmandu Bode (BD; 27.68°N - 85.39°E), Lumbini (LU; 27.49°N - 83.28°E), Dhaka University (DU; 23.72°N - 90.39°E), Myanmar (MY; 16.86°N - 96.15°E), Nghia Do (ND; 21.04°N - 105.80°E), Silpakorn University (SU; 13.81°N - 100.04°E), Ubon Ratchathani (UR; 15.24°N - 104.87°E), Vientiane (VI; 17.99°N - 102.57°E), Hong Kong Poly (HKP; 22.30°N - 114.18°E). (e) Simulated (BMAeroon) aerosol extinction coefficient (865 nm) (km^{-1}), averaged for 12°N - 30°N and spring 2013 (f) same as (e) but from OSIRIS measurements (750 nm). White contours in Fig (a)-(c) indicate the orography (km) of the Tibetan Plateau.

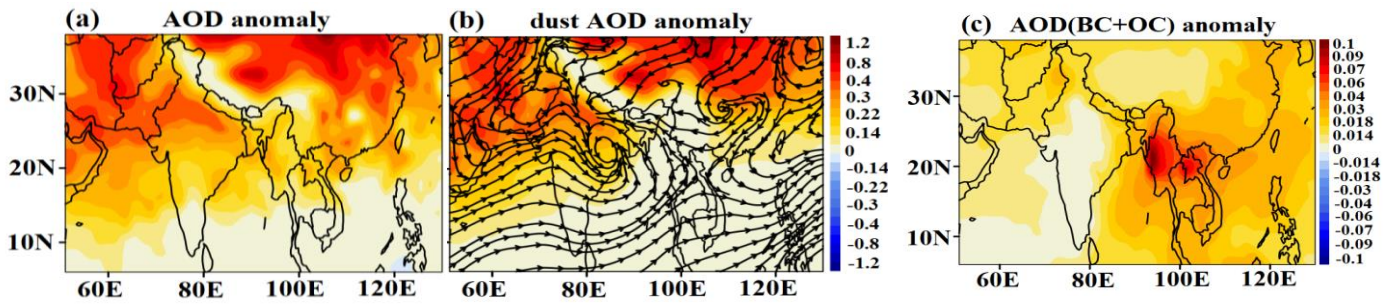


Figure 3: Distribution of ECHAM6-HAMMOZ simulated anomalies of (BMAeroon - BMAerooff) (a) AOD, (b) dust AOD, (c) BC-AOD and OC-AOD, together, averaged for spring 2013. Streamlines in figure 3b indicate wind anomalies at 900 hPa (BMAeroon-BMAerooff).

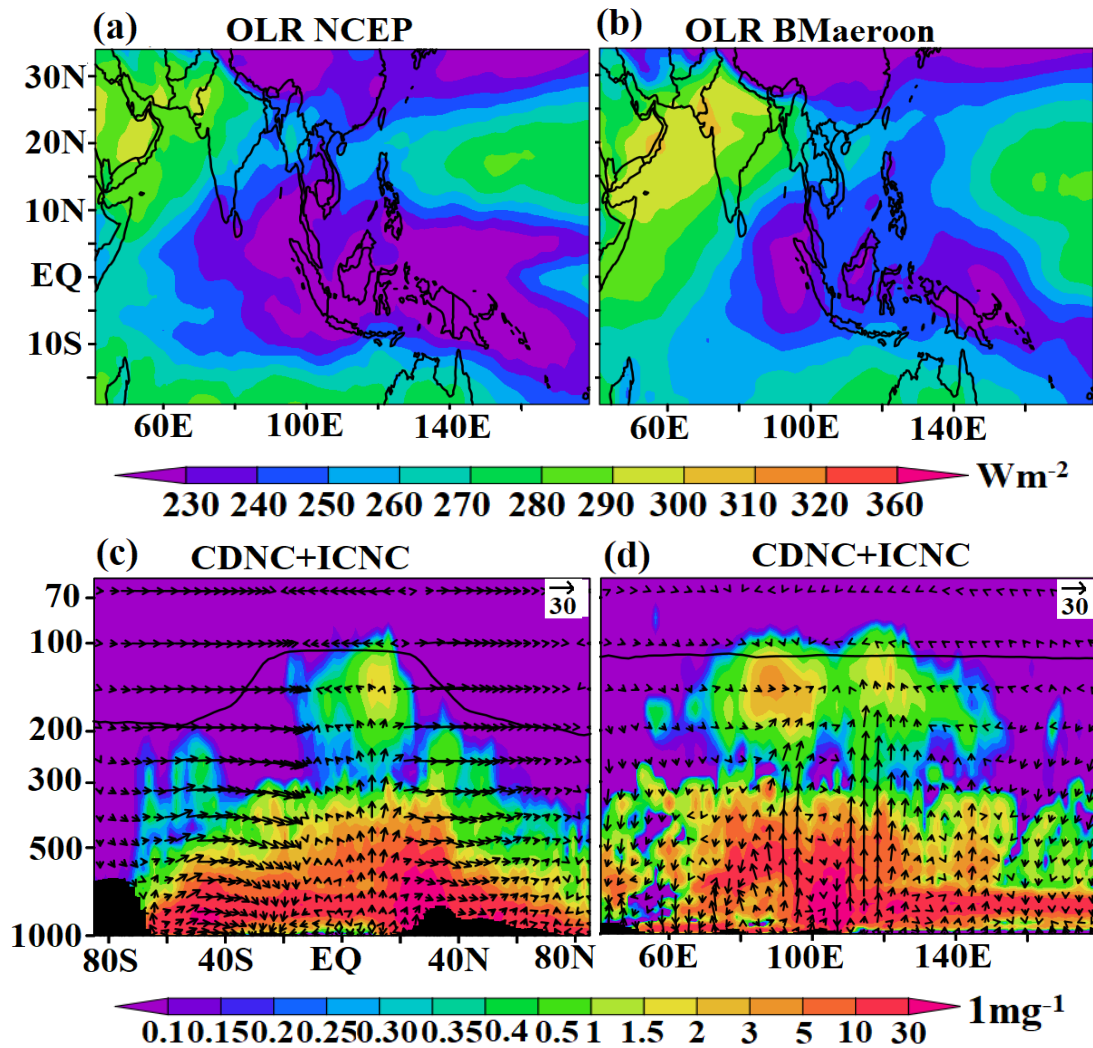


Figure 5: (a) Distribution of Outgoing Longwave Radiation (OLR) (W m^{-2}) from NCEP reanalysis-2 data averaged for spring 2013, (b) same as (a) but from the ECHAM6-HAMMOZ simulations (BMaeroon). Vertical distribution of cloud droplet number concentration (CDNC) and ice crystal number concentration (ICNC) (mg^{-1}) averaged for spring 2013 from ECHAM6-HAMMOZ simulations (BMaeroon) (c) latitude-pressure section (average for $85^{\circ}\text{E} - 140^{\circ}\text{E}$) and (d) longitude-pressure section (average for $10^{\circ}\text{N} - 20^{\circ}\text{N}$). Vectors of the circulation (BMaeroon) are shown in (c)-(d) with the vertical velocity field scaled by 300.

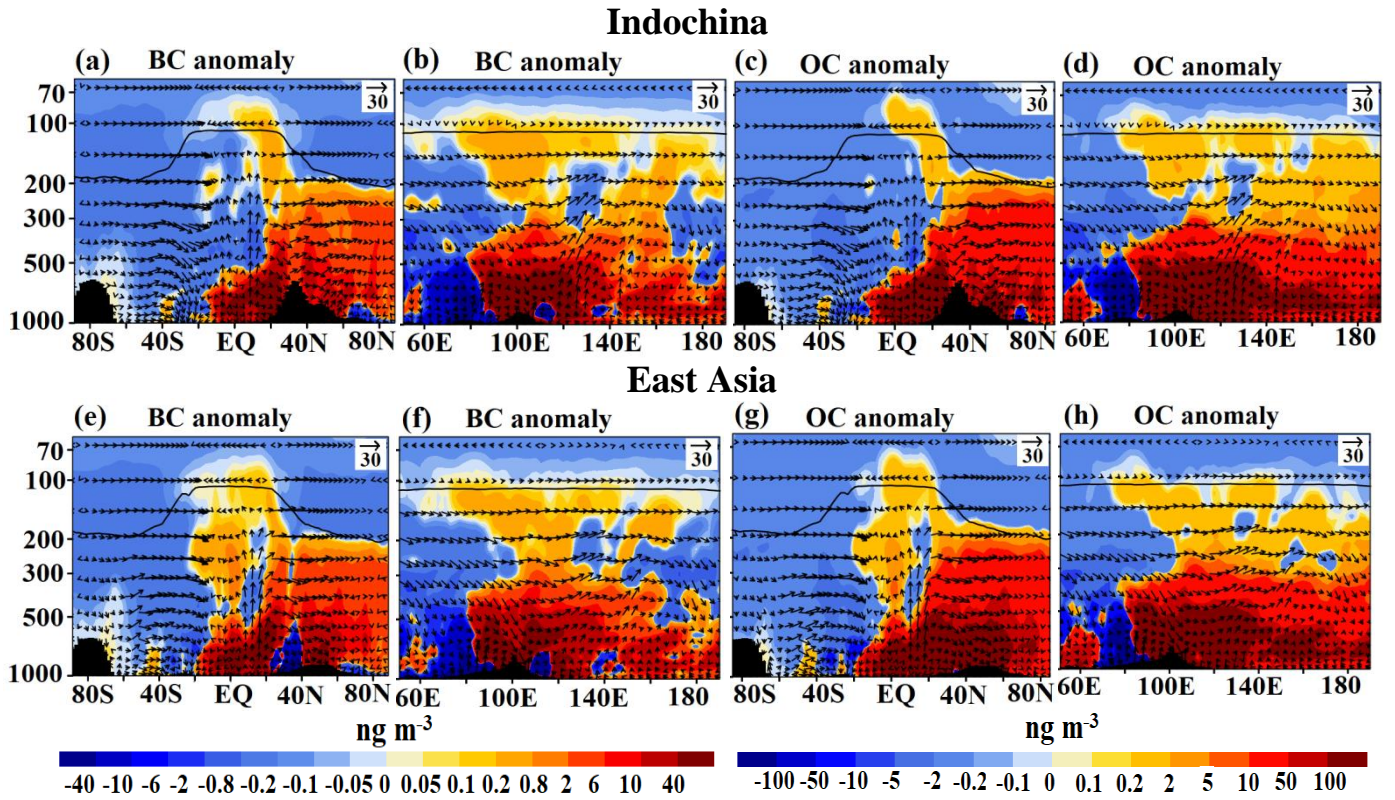


Figure 6: Vertical cross-section of anomalies of BC (ng m^{-3}) ($B_{\text{Maeroon}} - B_{\text{Maerooff}}$) averaged for the spring 2013 and (a) latitude-pressure section (averaged for 91°E - 107°E), (b) longitude-pressure section (averaged for 18°N - 24°N). (c-d) is the same as (a-b) but for OC. (e) same as (a) but averaged over 108°E - 123°E , (f) same as (b) but averaged for 18°N - 24°N . (g-h) same as in (e-f) but for OC. The arrows in (a-h) indicate winds in m s^{-1} with the vertical velocity field scaled by 300. The black vertical bar shows the topography and the black line indicates the tropopause.

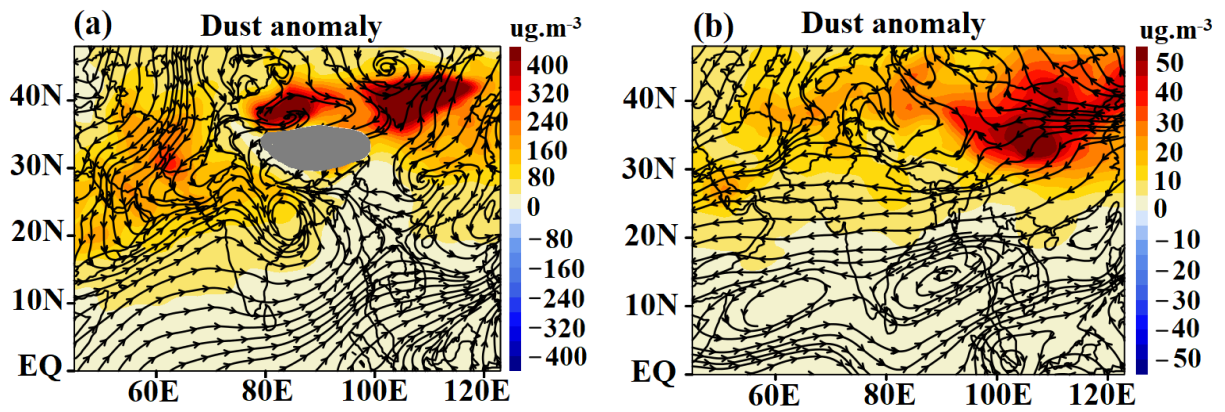


Figure S2: Distribution of anomalies of dust aerosol ($\mu\text{g}\cdot\text{m}^{-3}$) (BMaeroon-BMaerooff) averaged for spring 2013 for (a) the lower troposphere (1000 to 700 hPa) and (b) the mid-upper troposphere (600 hPa - tropopause). Gray shading in Fig (a) indicates the Tibetan Plateau.

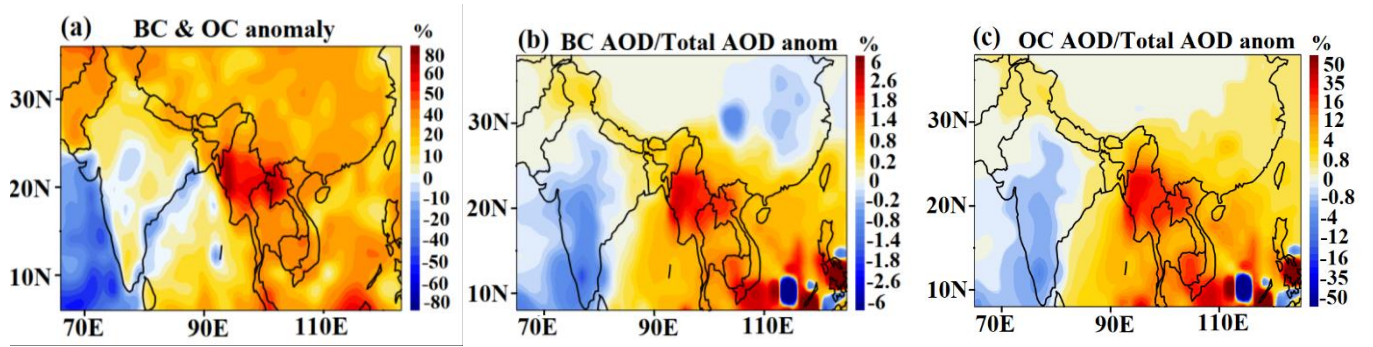


Figure S3: Distribution of anomalies ($B_{Maeroon} - B_{Maerooff}$) averaged for spring 2013 (a) atmospheric column concentration of BC and OC together (%), (b) ratio of BC-AOD to the total AOD (%), (c) ratio of OC-AOD to total AOD (%).